THE BELL SYSTEM TECHNICAL JOURNAL
Vol. 57, No. 5, May–June 1978
Printed in U.S.A.

An Earth-Space Propagation Measurement at Crawford Hill Using the 12-GHz CTS Satellite Beacon

By A. J. RUSTAKO, JR.

(Manuscript received September 26, 1977)

This paper describes a measurement of atmospheric attenuation and depolarization, primarily due to rain, of the 11.7-GHz cw beacon signal from the Communications Technology Satellite (CTS). This beacon source made possible the first fixed-path, nearly continuous measurements of earth-space propagation at this frequency. A measurement is being made at Bell Laboratories, Crawford Hill, in Holmdel, New Jersey using a fully steerable, 6-meter-aperture, horn-reflector antenna fitted with a dual-sense, circular-polarized feed. The amplitudes of the copolarized and cross-polarized components are measured with a two-branch, stable, narrowband, frequency tracking receiver. The receiving system, which was designed to run unattended, is described. Propagation data for a greater than 1-year period beginning April 1976 are presented. The attenuation data show that an outage time of $2^1/_2$ hours per year can be expected for a 10-dB rain fade margin. Significant anomalous depolarization effects not directly related to rainfall have been observed.

I. INTRODUCTION

The launch of the CTS satellite has provided a useful signal source for earth-space propagation experiments. The interest is in measuring long-term (approximately one year) atmospheric attenuation and depolarization, primarily due to rain. The satellite carries a cw beacon at a frequency of 11.7 GHz with a nominal output power of 200 mW. The satellite beacon antenna is a right-hand sense, circularly polarized, earth-coverage horn with an axial ratio of 1.5 dB within an enclosed beam

angle of 17 degrees. The satellite is in geosynchronous orbit and is located nominally at 116°W longitude with an inclination of less than 1 degree.

A disadvantage in using the CTS satellite beacon for these measurements is that the beacon is turned off during the spring and fall eclipse periods when the solar cell panels are shadowed by the earth. In the fall 1976 eclipse, the beacon was turned off completely for seven weeks. Fortunately, few significant rain events occurred during this time. In the spring 1977 eclipse, the beacon was turned off for only short periods, approximately one hour each day over a six-week period.

The rain attenuation data for these eclipse periods were bridged by statistically scaling data from a colocated 19-GHz COMSTAR A beacon measurement. This scaling technique is described in the appendix to this paper.

The Crawford Hill receiving system is located in Holmdel, New Jersey at approximately 74°W longitude and 40°N latitude. For this location, the receiving antenna point is nominally at an azimuth angle of 234 degrees with an elevation of 27 degrees. This provides approximately a 20-km path through atmospheric rain showers. The signal parameters for this path are shown in Table I. The clear air carrier-to-noise ratio in the copolarized signal branch is 43.4 dB in a 32-Hz bandwidth. The cross-polarization signal level for clear air is typically 33 dB below the copolarized signal level. A 28.5-dB carrier-to-noise ratio in the cross-polarized signal branch is obtained by detection in a 0.5-Hz bandwidth.

The Crawford Hill receiver provides a continuous measure of both the copolarized received signal and the cross-polarized component due to rain or other atmospheric effects.[1] The entire system is normally unattended and takes data continuously on a 24-hour basis.

II. ANTENNA AND TRACKING

The receiving antenna is a fully steerable horn reflector[2] with a 6-meter aperture. Figure 1 is a photograph of the antenna. The antenna feed structure, receiver, and recording system are located within the vertex cab of the horn. The antenna has a hybrid-coupled, orthogonal feed to provide two isolated signal signal components to the receiver. One port provides the right-hand circular copolarized component and the second provides the left-hand cross-polarized component. The measured isolation of these two output ports using the satellite beacon is greater than 33 dB on axis for clear-air propagation conditions.

The receiving antenna has a gain of 57 dB and a 3-dB beamwidth of approximately 0.3 degree. The narrow beamwidth necessitates continual antenna pointing to track the diurnal satellite motion. The antenna is pointed by an open loop technique[3] using predicted azimuth and ele-

Table I — Path parameters for CTS satellite

Beacon transmitter power ≧ 200 mW	≧ −7.0 dbW
Antenna gain toward Crawford Hill	= +18.4 dB
ERP	= +11.4 dBW
Path loss (38982 km) to Crawford Hill	= 205.6 dB
Clean air attenuation	= 0.3 dB
Net loss	= 205.9 dB
Horn reflector antenna gain	= 57 dB
Received signal power	= −137.5 dBW
	= −107.5 dBm
Ground Receiver	
Receiver T_E = 1150K, kTF	= −166 dBm/Hz
Copolarized received signal C/N density	= 58.5 dB/Hz
Copolarized signal C/N ratio in 32 Hz bandwidth (clean air)	= 43.4 dB
Residual cross-polarized level below copolarized received signal (clear air)	= −33 dB
Cross-polarized signal C/N ratio in 0.5 Hz bandwidth (clear air)	= 28.5 dB

vation data supplied by NASA. The overall antenna servo pointing accuracy is estimated to be better than ±0.03 degree.

III. RECEIVER DESIGN

The receiver is composed of two branches. One branch measures the amplitude of the copolarized signal, the second measures the relatively weak cross-polarized signal. The copolarized signal branch is used to

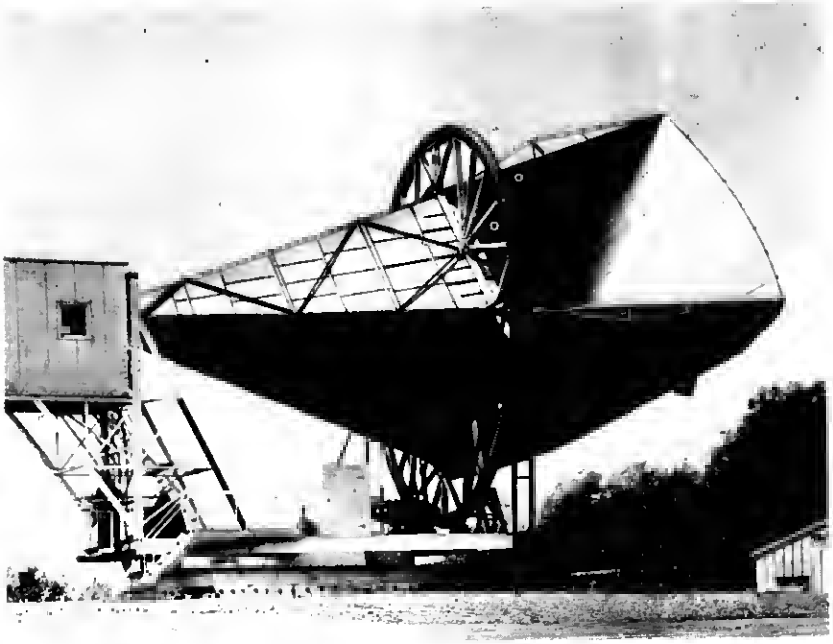

Fig. 1—Six-meter horn reflector antenna.

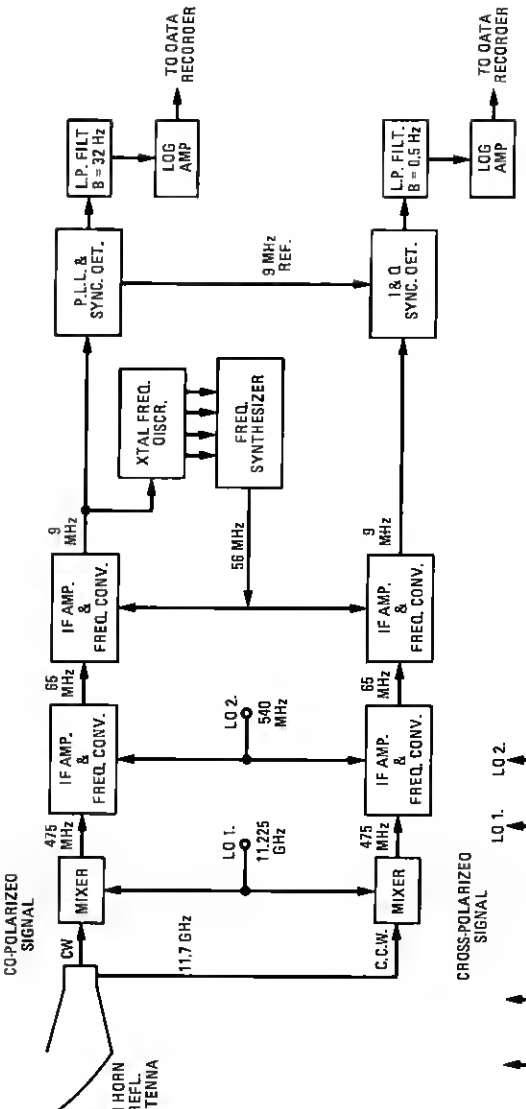

Fig. 2—CTS beacon measuring receiver.

control frequency tracking and provide a phase reference for detection in the cross-polarized signal branch. Figure 2 is a block diagram of the CTS beacon measuring receiver. Each receiver branch uses multiple heterodyning to convert the 11.7-GHz input frequency from the satellite to a final IF frequency of 9 MHz where envelope detection is carried out. The 9-MHz IF signal in each branch is bandpass-filtered through a 500-Hz wide crystal filter. The 9-MHz IF output from the copolarized signal branch is split, with one portion used for frequency control and the other envelope-detected. The frequency control component is envelope-limited to provide an input to a frequency discriminator. The second 9-MHz IF component is envelope-detected using a phase-locked synchronous detector. The detector output is low-pass filtered, its logarithm taken and recorded.

The phase-locked 9-MHz reference signal for the copolarized synchronous detector is split to provide a reference signal for in-phase and quadrature detection of the cross-polarized branch, 9-MHz IF signal. The outputs from these detectors are separately low-pass filtered and vectorially summed. The logarithm of the summed output is taken, then recorded.

A detailed block diagram of the receiver automatic frequency tracking control is shown in Fig. 3. The components in the control loop are an envelope limiter, a temperature-controlled crystal frequency discriminator, a gated integrator, a window comparator, a gated clocked up-down counter, and a BCD controlled frequency synthesizer with frequency doubler. The slow-frequency variation of the satellite beacon signal (~5 kHz/day) is tracked by measuring the change in the copolarized 9-MHz IF signal frequency and controlling the nominal 56-MHz local oscillator frequency to return the IF signal to exactly 9 MHz. A portion of the copolarized 9-MHz IF signal is envelope-limited to provide an input to a quartz crystal frequency discriminator. The discriminator output is integrated to smooth short-term variations and applied to the window voltage comparator. The window voltage comparator determines if the discriminator input frequency has changed beyond a preset allowable amount. The comparator gates a clock signal that either increases or decreases the count in a digital register. A BCD output from the digital register drives the frequency control of a programmable frequency synthesizer. The frequency synthesizer output at about 28 MHz is frequency-doubled to 56 MHz to provide a local oscillator for the 65-MHz to 9-MHz frequency conversion.

A clock frequency of 1 Hz is used to drive the digital register. With this clock frequency and the synthesizer frequency doubling, the receiver will track an input frequency rate of change of 2 Hz per second. This has been found adequate for the beacon frequency drift rates encountered.

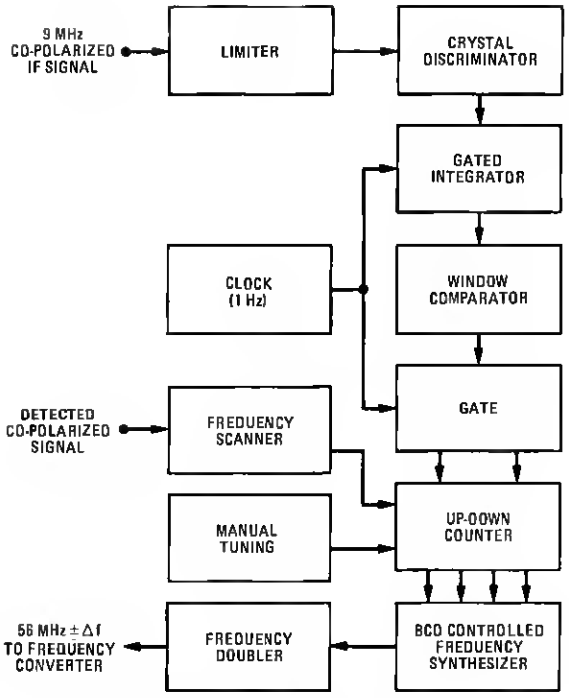

Fig. 3—Automatic frequency tracking control.

The use of the digital register-frequency synthesizer technique provides an automatic-frequency control with memory.[4] If the received beacon signal is lost because of a deep fade, beacon turnoff, or tracking malfunction, the receiver remains tuned to the beacon frequency preceding the loss and will not normally change frequency until the signal returns. The automatic frequency tracking control is provided with a frequency scan circuit to retune the receiver automatically if the beacon signal is lost and later appears outside the 500-Hz receiver bandwidth. This occurs during eclipse periods when the satellite power is shut down. The beacon oscillator cools and changes frequency by several kilohertz. The receiver frequency scan is delayed about 3 minutes on loss of signal, then proceeds to scan at a 100-Hz-per-second rate approximately 8 kHz either side of the last known beacon frequency. This scan technique has provided rapid reacquisition of the beacon signal during eclipse.

The overall frequency of the receiver is controlled by a single 10-MHz stable crystal oscillator in conjunction with several frequency multiplier chains. The crystal oscillator has a short-term (1 s) stability of 1×10^{11} and an aging rate of $<1.5 \times 10^{-7}$/year. Figure 4 is a block diagram of the oscillator and multiplier chains. The first local oscillator at 11.225 GHz

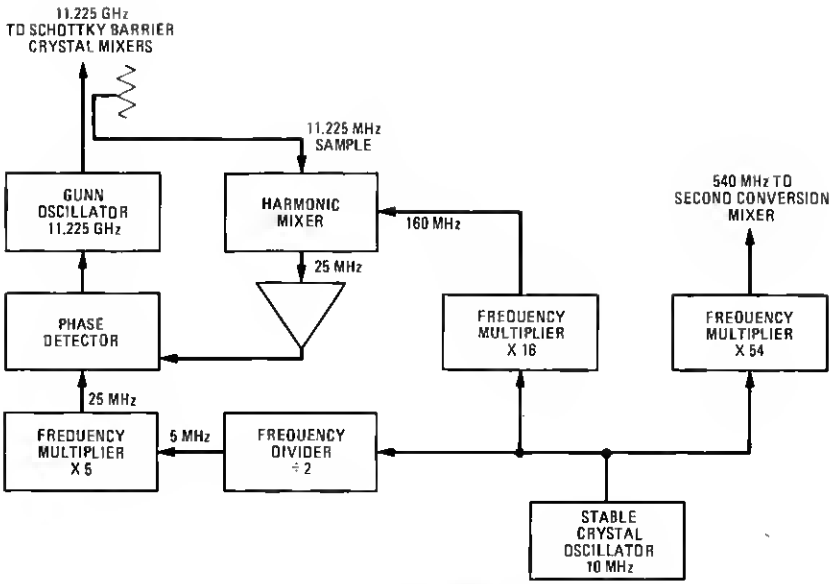

Fig. 4—Receiver local oscillator chain.

is obtained from a phase-locked, varactor-tuned, Gunn diode oscillator. The Gunn oscillator output is heterodyned with a stable reference signal at 160 MHz in a harmonic mixer. The frequency difference is limited and compared in phase with a second reference signal at 25 MHz. An error signal from the phase detector is fed back to the Gunn oscillator frequency control. The second local oscillator at 540 MHz is directly obtained from frequency multiplication of the stable crystal oscillator.

Figure 5 is a detailed block diagram of the synchronous envelope detectors in both receiver branches. A detection reference signal is provided by a 9-MHz, voltage-controlled crystal oscillator. This VCXO is phase-locked to the 9-MHz limiter output in the frequency control of the co-polarized branch. The 9-MHz IF output signal from the copolarized branch is synchronously envelope-detected and low-pass filtered. A bandwidth of 32 Hz is provided by an active 4-pole Butterworth low-pass filter. The signal envelope output from the low-pass filter is passed through a baseband log amplifier to the data recorders. The parameters of the log amplifier are set to provide a 40-dB dynamic range.

The 9-MHz IF output signal from the cross-polarized branch is envelope-detected by in-phase and quadrature detectors. The detected in-phase and quadrature components are low-pass filtered and vectorially summed to provide a single output proportional to the magnitude of the cross-polarized signal. A bandwidth of 0.5 Hz is provided by active 4-pole Butterworth low-pass filters. The combined output is passed

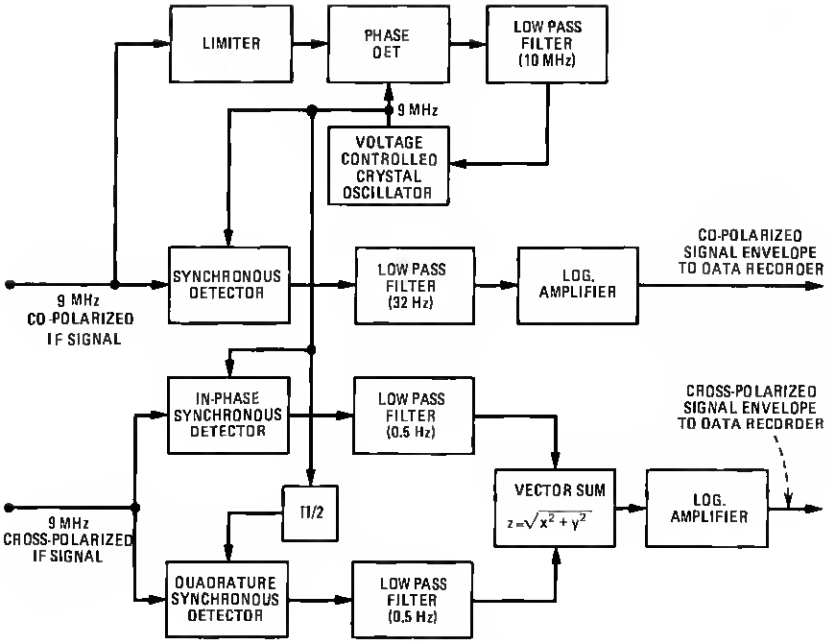

Fig. 5—Synchronous envelope detectors.

through a baseband log amplifier to the data recorders. The parameters of the log amplifier are again set to provide a 40-dB dynamic range.

The receiver and data recorder are calibrated by providing a stable input signal at 11.7 GHz to the receiver input mixers. This calibration source is obtained by frequency multiplication of a synthesized signal source wbich is referenced to the 10-MHz stable crystal oscillator. The calibration source was carefully shielded to prevent stray signal leakage to the receiver. The calibration source output, controlled by a precision waveguide attenuator, is coupled into waveguide switches at the receiver inputs.

IV. MEASUREMENT RESULTS

The beacon measuring system has been operational since April 1976. Nearly continuous measurements have been made of the coplarized and cross-polarized components from tbe satellite beacon signal. Data are presented for greater than a 1-year period beginning April 1976. During this time, some data were lost during the fall and spring eclipse periods when the satellite beacon was turned off to conserve battery power. A small amount of data was also lost due to an antenna servo malfunction. The copolarized signal data were analyzed for a one-year period to obtain attenuation statistics. Using data for attenuation greater than 1 dB, a

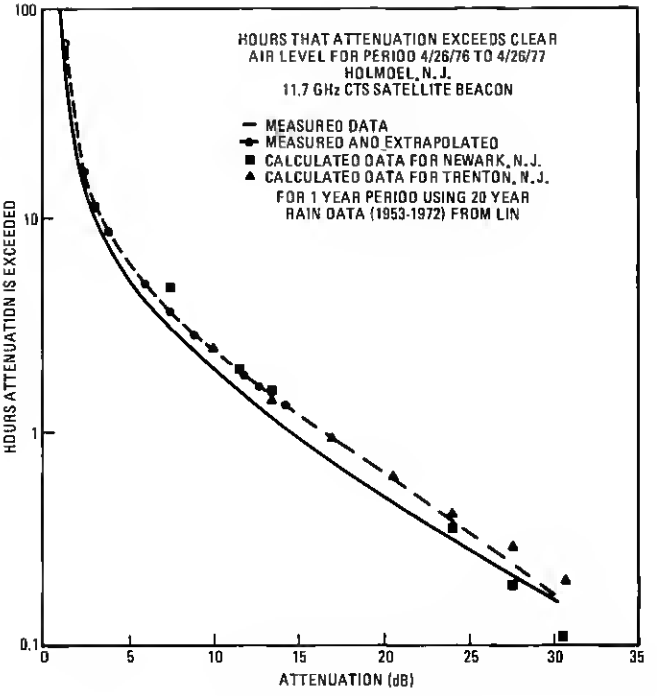

Fig. 6—Cumulative attenuation statistics for April 26, 1976 to April 26, 1977.

distribution curve showing the time an attenuation greater than clear air was exceeded versus attenuation is plotted as the solid line in Fig. 6. This curve shows data for the one-year period excluding eclipse outage time. A second curve, the broken line in Fig. 6, shows the effect of bridging the outage periods with data scaled from a simultaneous 19-GHz COMSTAR A beacon measurement. The frequency scaling, described in the appendix, relates measured attenuation statistics at the two frequencies during a common time to predict attenuation statistics at 12 GHz when the CTS beacon signal was lost. The 12-GHz statistics could be predicted up to approximately 14 dB corresponding to the 40-dB threshold in the COMSTAR A data. Beyond 14 dB, the 12-GHz distribution curve, shown dashed, asymptotically approaches the measured curve since heavy rain with attendant high attenuation did not occur during the bridged periods. In general, for practical system design, the attenuation statistics are of greatest interest for attenuation less than 14 dB.

The bridged curve represents a reasonably good estimate of the attenuation statistics for the full year. The curve therefore could be useful in estimating the outage time of a satellite communications link given

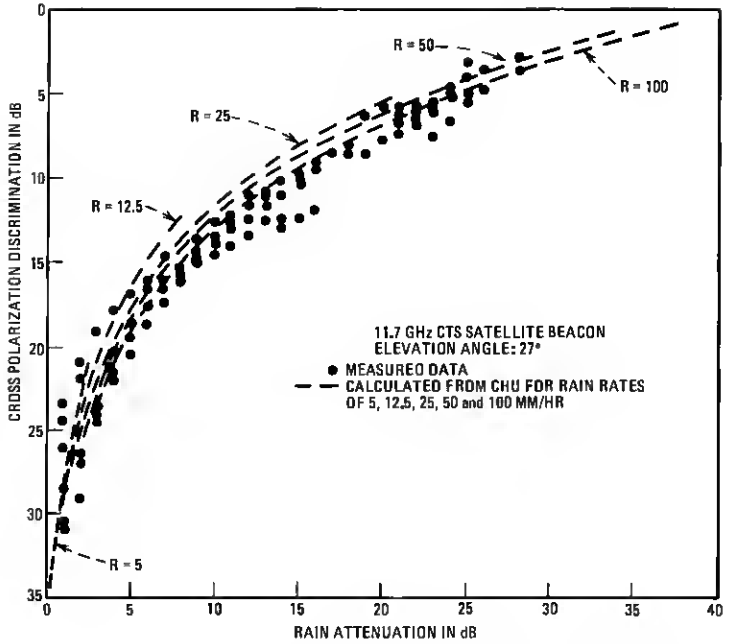

Fig. 7—Cross polarization discrimination as a function of rain attenuation.

an attenuation or fading margin. For example, a system with a 10-dB margin would have had a 2½-hour outage time over the year period.

The distribution curve shows a change in slope as attenuation increases. At low attenuation, the logarithmic change in outage time is very rapid with incremental decibel changes in attenuation. Above about 10-dB attenuation, the slope appears to be fairly constant, indicating there is a decreasing rate of return in outage time with an increase in attenuation or fading margin. Therefore, unless a much lower outage time is required for a particular service, a margin of about 10 dB may be optimum.

In addition to the experimental result, Fig. 6 shows several calculated points of an attenuation distribution obtained from Lin.[5] The calculation was based on five-minute point rain rate data for a 20-year period (from 1953 to 1972) for Newark and Trenton, New Jersey for a path elevation angle of 27 degrees. These points show the average number of hours per year that an attenuation is exceeded for a similar path at these two locations. Very close agreement can be observed between the measured and calculated data.

The cross-polarization data were analyzed for several rain events during tbe measurement period. The cross-polarization discrimination, defined as the decibel difference between the desired and undesired

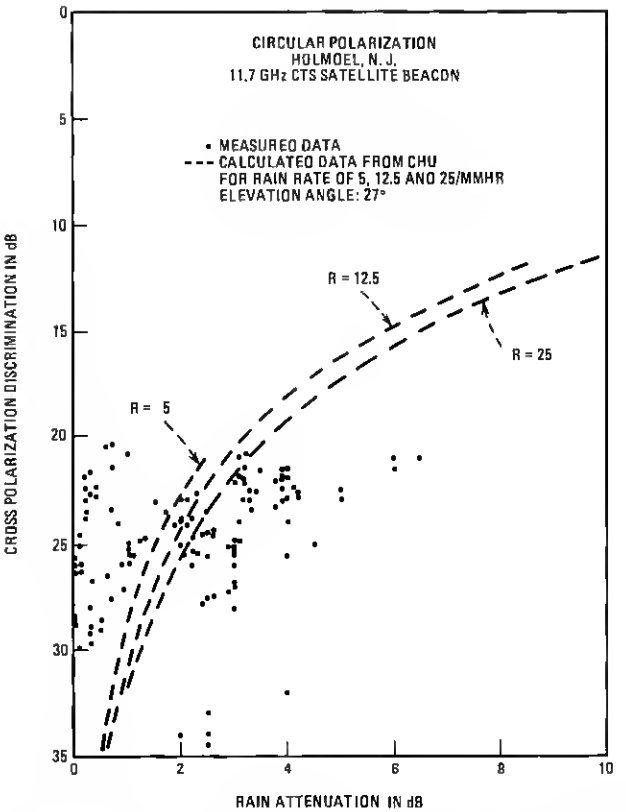

Fig. 8—Cross polarization discrimination as a function of rain attenuation.

polarization components, was measured as a function of rain attenuation. Data for two types of rain events are shown in Figs. 7 and 8. In Fig. 7, measured data shown as dots are for three events during August 1976 where high rain rates were encountered. The cross-polarization discrimination was measured for copolarized signal attenuations 1 dB or greater than clean air. The measured data show a decrease in discrimination with increasing path attenuation. For example, at a 10-dB attenuation the undesired cross-polarized components are approximately 14 dB below the copolarized signal and at 20-dB attenuation the discrimination has decreased to about 8 dB. In addition to the measured data, five calculated curves of cross-polarization discrimination are shown. These curves from Chu[6] were calculated from differential attenuation and phase shift through oblate spheroidal raindrops at 12 GHz for five rain rates. A maximum path length of 20 km, an elevation angle of 27 degrees, and a single uniform rain-canting angle were assumed. These curves represent an upper bound of the theoretical cross-polar-

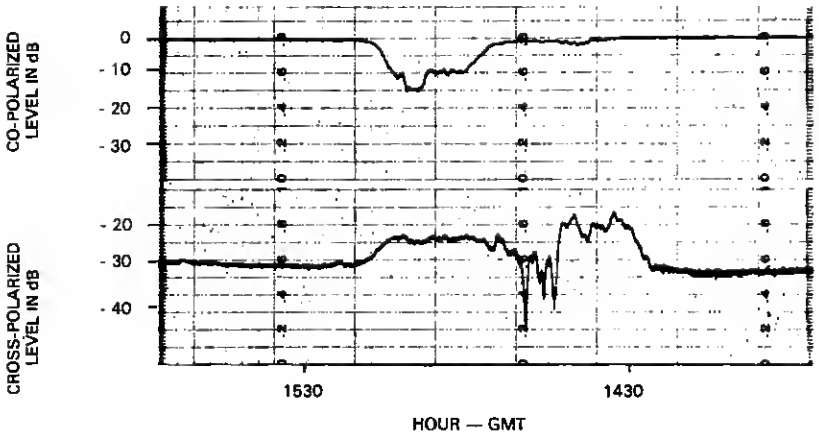

Fig. 9—Anomalous cross polarization event, 11.7 GHz CTS beacon, Holmdel, N.J., August 8, 1976.

ization discrimination. A reasonably good fit is shown between Chu's theory and the measured data for copolarized signal attenuation greater than 5 dB. The measured data generally fall below Chu's curves by a few dB, which could be caused by randomness in rain-canting angle as would be normally by expected with wind-driven rain.

Similar data are plotted in Fig. 8 for three rain events during April, May, and June 1977. The events of this period were of low rain rate compared to the August data and therefore the copolarized signal fading was small, less than 7 dB. The cross-polarization discrimination was measured for copolarized signal attenuation as low as 0.1 dB greater than clean air. The measured data show considerable scatter with little resemblance to Chu's curves. This scatter might be due to ice or atmospheric turbulence effects that are hidden in the more intense summer rains.

In addition to the normally expected strong depolarization effects with rain attenuation, some anomalous effects not predicted by contemporary rain propagation theory have been observed. One effect, which has been reported elsewhere,[1] is a large change in cross-polarization discrimination without an attendant measurable change in copolarization signal attenuation. A graphic example of one event is shown in Fig. 9. This segment of a pen recording shows a simultaneous time trace of the right-hand circular copolarized and the left-band circular cross-polarized signal components. The decibel levels shown are relative to the clear air copolarized signal level. Significant variation in depolarization was observed in the vicinity of 1430 hours when the copolarized signal is at its clear air level. This effect has been observed both during summer rain events, often related to thunderstorms, and during the cooler months

with only an overcast sky, near-freezing temperature, and no precipitation. This effect is very likely caused by differential phase shift through ice crystals present in the propagation path.

A second observed anomalous depolarization effect has been rapid discrete steps in the cross-polarized signal during thunderstorms. This effect, shown in the cross-polarized trace in Fig. 10, is believed due to rapid orientation of ice crystals in the transmission path by lightning discharges near the path.[7]

Both these anomalous effects have been simultaneously observed over similar transmission paths using the COMSTAR A and B beacon signals at 19 and 28 GHz.

V. SUMMARY

A measurement of atmospheric attenuation and depolarization at 12 GHz over an earth-space propagation path has been described. The measurement system uses a two-branch, narrowband frequency tracking receiver in conjunction with a 6-meter-aperture, horn-reflector antenna to measure copolarized and cross-polarized components of the received cw beacon signal from the Communications Technology Satellite.

The measurement system has been operating essentially unattended since April 1976, recording the atmospheric attenuation and depolarization of the satellite beacon signal. Attenuation statistics showing a distribution of the number of hours the path attenuation exceeded the clear air level have been presented for a one-year period. The distribution was corrected for data loss when the 12-GHz beacon signal was unavailable during eclipse by bridging scaled statistical data from a colocated 19-GHz COMSTAR A beacon measurement. The distribution shows that a 12-GHz satellite communication link with an attenuation or fading margin of 10 dB would experience a $2\frac{1}{2}$-hour outage time in a one-year period.

Depolarization effects have been observed during normal rain fade events and when no measurable copolarized signal attenuation was present. The depolarization effects observed for rain attenuation greater than 5 dB appear to follow predictions based on differential attenuation and phase shift through oblate spheroidal rain drops. However, when no measurable or very low copolarized signal attenuation is present, the observed depolarization effects are very likely caused by differential phase shift through ice crystals.

VI. ACKNOWLEDGMENTS

I want to acknowledge useful discussion with H. W. Arnold, T. S. Chu, D. C. Cox, S. H. Lin, D. O. Reudink, and R. W. Wilson. I am also indebted to H. W. Arnold for providing his data analysis programs and the COM-

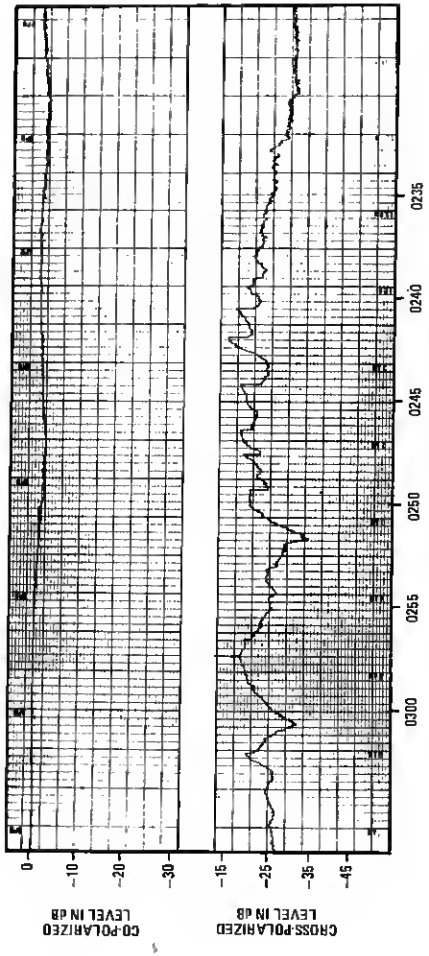

Fig. 10—Anomalous cross polarization event, 11.7 GHz CTS beacon, Holmdel, N.J., April 25, 1977.

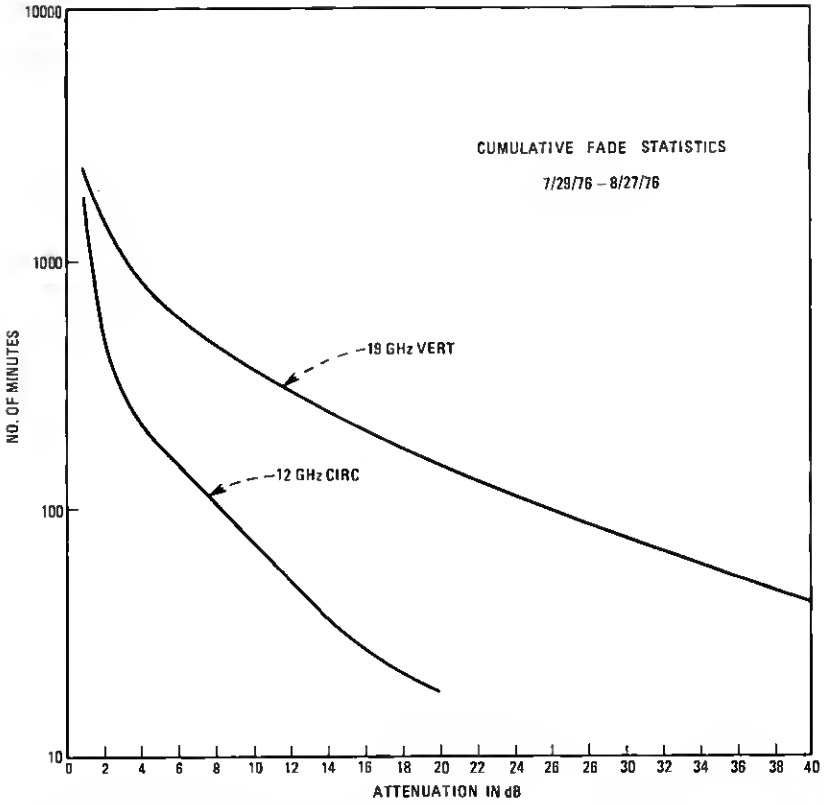

Fig. 11—Cumulative attenuation statistics at 12 and 19 GHz for July 29, 1976 to August 27, 1976.

STAR data, A. W. Norris for his continuing assistance in the operation of the receiving system, and H. R. Hunczak at NASA Lewis Research Center for providing CTS tracking data.

APPENDIX

Frequency Scaling of Attenuation Statistics

To obtain an estimate of the attenuation statistics at 12 GHz when the CTS beacon signal was lost during eclipse periods and system outage, an empirical relation was determined between the 12-GHz attenuation statistics and 19-GHz COMSTAR beacon attenuation statistics.

The propagation paths through the atmosphere from the two satellites and the signal polarizations are different. The CTS beacon signal is circularly polarized and at Holmdel requires a ground station antenna point at approximately 234 degrees azimuth and 27 degrees elevation. The

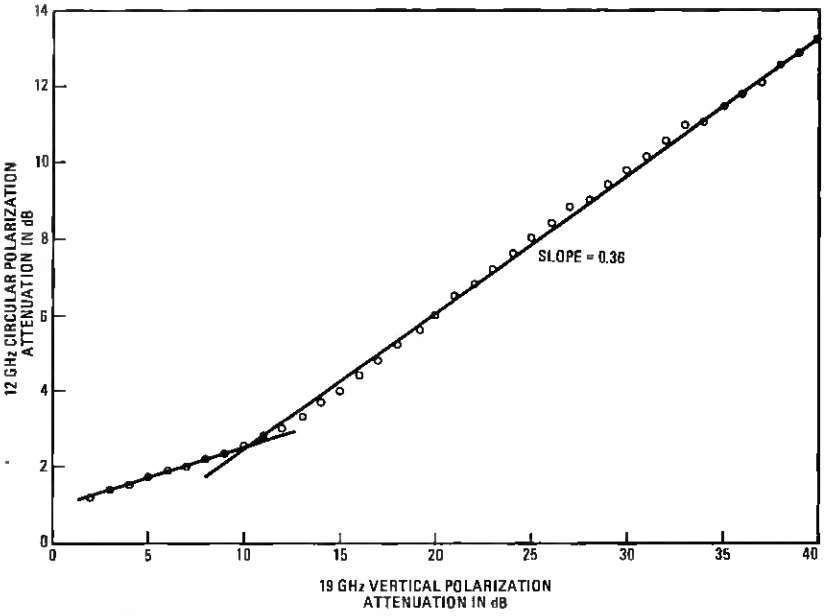

Fig. 12—Plot of 12-GHz attenuation as a function of 19-GHz attenuation at constant outage periods for July 29, 1976 to August 27, 1976.

COMSTAR A beacon signal is linearly polarized and requires an antenna point of approximately 244 degrees azimuth and 18 degrees elevation. The frequency scaling presented here, therefore, only applies to these two experiments.

The frequency scaling of the attenuation statistics was done by relating the decibel levels of the 12- and 19-GHz cumulative attenuation distribution curve at equal outage times. A common measurement period was chosen when both systems were operating and where sufficient rainfall occurred to produce significant attenuation at the two frequencies. This period, between July 29 and August 27, 1976, included several rain events, providing an ensemble average over multiple events. Figure 11 shows the measured cumulative attenuation statistics at 12 and 19 GHz. Using the data from this figure, another curve was plotted showing the attenuation at 12 GHz as a function of attenuation at 19 GHz at constant outage times. This frequency relationship is shown in Fig. 12. This curve appears to have segments with two distinctly different slopes. The change in slope at lower attenuations may be due in part to digitizing errors of the 12-GHz data. In the region above 10 dB attenuation at 19 GHz, the curve has a constant slope of 0.36. This shows, for a given outage time, the attenuation observed at 12 GHz will be 0.36 times the decibel attenuation at 19 GHz for the same measurement period.

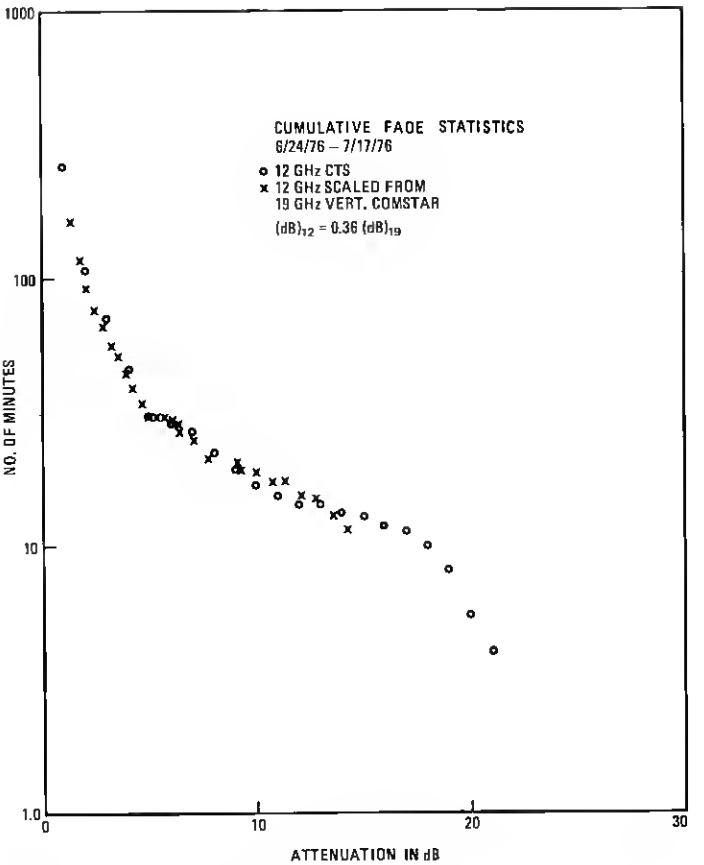

Fig. 13—Cumulative attenuation statistics at 12 GHz with data scaled from 19 GHz for June 24, 1976 to July 17, 1976.

To test the accuracy of this rule, another period of data was analyzed. The cumulative attenuation statistics for 12 and 19 GHz were calculated for the period between June 24 and July 17, 1976. The 19-GHz data were scaled to 12 GHz using the previously determined factor. Both data are plotted in Fig. 13. The two sets of data are almost indistinguishable over most of the distributions, which lends reasonable confidence to the scaling technique.

REFERENCES

1. D. C. Cox, H. W. Arnold, and A. J. Rustako, Jr., "Some Observations of Anomalous Depolarization on 19 and 12 GHz Earth-Space Propagation Paths," Radio Science, *12*, No. 3 (May–June 1977), pp. 435–440.
2. A. B. Crawford, D. C. Hogg, and L. E. Hunt, "A Horn-Reflector Antenna for Space Communications," B.S.T.J., *40*, No. 4 (July 1961), pp. 1095–1116.

3. P. V. Bradford and R. W. Wilson, "Fourier Series Representation for Tracking Inclined, Elliptical, Synchronous Satellite Orbits," private communication.
4. H. W. Arnold, private communication.
5. S. H. Lin, private communication.
6. T. S. Chu, "Rain-Induced Cross-Polarization at Centimeter and Millimeter Wavelengths," B.S.T.J., *53*, No. 8 (October 1974), pp. 1557–1579.
7. N. J. McEwan, P. A. Watson, A. W. Dissanayake, D. P. Haworth, and V. T. Vakili, "Cross-Polarisation From High-Altitude Hydrometeors on a 20 GHz Satellite Radio Path," Electronics Letters, *13*, No. 1 (January 6, 1977), pp. 13–14.